



ELSEVIER

Available online at www.sciencedirect.com

SCIENCE @ DIRECT®

Nuclear Physics A 729 (2003) 867–883

NUCLEAR
PHYSICS A

www.elsevier.com/locate/npe

Light-neutrino mass spectrum, nuclear matrix elements, and the observability of neutrinoless $\beta\beta$ decay

O. Civitarese^{a,*}, J. Suhonen^b

^a *Department of Physics, University of La Plata, c.c. 67 (1900), La Plata, Argentina*

^b *Department of Physics, University of Jyväskylä, P.O. Box 35, FIN-40014 Jyväskylä, Finland*

Received 28 March 2003; received in revised form 1 October 2003; accepted 6 October 2003

Abstract

Parameters which describe neutrino flavor oscillations and neutrino mixing mechanisms, obtained from the analysis of the Sudbury Neutrino Observatory (SNO), Super-Kamiokande (SK), CHOOZ, KamLAND and WMAP data, are used to calculate upper limits of the effective neutrino mass (m_ν) relevant for the neutrinoless double-beta decay ($0\nu\beta\beta$). The observability of planned $0\nu\beta\beta$ experiments, and the present status of the decay of ^{76}Ge are discussed within different light-neutrino mass spectra and by presenting a systematics on the available nuclear matrix elements.

© 2003 Elsevier B.V. All rights reserved.

PACS: 14.60.Pq; 23.40.Bw; 23.40.Hc

Keywords: Neutrino mass; Neutrino-mass hierarchy; Neutrinoless double-beta decay; Nuclear matrix elements

1. Introduction

The present understanding about the properties of the neutrino has been dramatically advanced by the results of various large-scale experiments, as reported by SNO [1], SK [2], KamLAND [3], CHOOZ [4], and WMAP [5] Collaborations. These experimental evidences have confirmed the existence of neutrino flavor oscillations and have established stringent limits to the neutrino mass-mixing mechanisms. A general overview of the latest experimental results is given in review articles by Valle [6], Bahcall et al. [7]. Detailed

* Corresponding author.

E-mail address: civitarese@fisica.unlp.edu.ar (O. Civitarese).

discussions about the extracted values of the mixing angles, mixing amplitudes, and mass differences can be found in Refs. [9–11]. The implications of the latest results on the physics of electroweak interactions and dark-matter studies have been discussed in Refs. [12–14].¹

In addition to the findings on neutrino flavor oscillations and the confirmation of some of the theoretically predicted possibilities for the mixing and enhancement of the oscillations in the presence of matter [15], double-beta-decay experiments [8] can provide complementary information on the nature of the neutrino and about its absolute mass scale [16–20]. This is a unique feature of the double-beta decay, which must be consistent with other scale-fixing measurements, like the WMAP measurements [5]. In the case of double-beta-decay measurements the knowledge about relevant nuclear matrix elements is crucial, as it is crucial to know the correct neutrino-mass spectrum for the analysis of the other type of measurements. The implications of the results of the solar, atmospheric, reactor and astrophysical neutrino experiments upon double-beta-decay experiments have been stated already in several publications, see, for instance, [21–26]. To the wealth of parameters involved in the analysis, like CP-phases, mixing angles and masses, one should add the nuclear-structure degree of freedom needed to extract the effective electron–neutrino mass [17–20].

At first glance, to physicists who are less familiar with nuclear-structure analysis, it may seem an easy task to produce the needed nuclear-structure information. Unfortunately it is not so because of several reasons:

- (a) double-beta-decay transitions take place in medium- and heavy-mass systems, where explicit shell-model calculations are unfeasible, unless severely truncated valence spaces are used;
- (b) results of the calculations depend on the structure of the double-odd-mass nucleus involved in the decay. These intermediate states play an essential role in the second-order transition matrix elements entering the expression of the decay rate, and less is known about them, as compared with the relatively large amount of information gathered about the spectrum and electromagnetic and particle-transfer transitions in double-even-mass nuclei. However, this dependence can be mimicked by a suitable choice of the average energy in the closure approximation. The use of closure is not justified for the case of the two-neutrino double-beta decay mode. Therefore, the value of the average excitation energy, in the case of the neutrinoless double-beta decay mode, may be taken as an additional parameter;
- (c) in dealing with medium- and heavy-mass nuclei one is forced to introduce approximations to obtain the participant wave functions and these approximations are not unique, they vary from model to model;
- (d) to assign a certain degree of significance to the already existing theoretical results one has to define, first, what should be taken as the equivalent of the experimental

¹ Because of the large amount of publications in the field we focus our attention on the most recent ones, since most of the valuable previous literature has been quoted in the papers which we have included in the present list of references.

confidence level, e.g., which models may be taken as references and what would be the confidence level assigned to them depending upon the used approximations.

In the past, all of these features have been referred to as the *uncertainties* in the nuclear matrix elements and roughly estimated to be within factors of 2 to 3, with respect to some reference values. This aspect of the problem certainly deserves some attention, as we are going to discuss later on in this work, since there turns out to be a gap between the range of mass limits extracted from double-beta-decay studies, 0.4 eV to 1.3 eV [22], and those extracted from the other neutrino-related studies which yield upper limits of the order of 0.10 to 0.20 eV [24] or even lower [12]. There is a clear discrepancy between both sets of results concerning the observation of neutrinoless double-beta ($0\nu\beta\beta$) decay. This issue has become a hot one, due to the recent claim [27] about the positive identification of neutrinoless-double-beta decay signals in the decay of ^{76}Ge (see, however, the objections presented in [28–30]), from which a central value of the mass of the order of 0.39 eV was extracted [27]. We think that these aspects must be considered from the point of view of both neutrino- and nuclear-structure physics. In this work we discuss the constraints set by the oscillation and mass parameters on the effective neutrino mass relevant for the $0\nu\beta\beta$ decay, and compare them with the ones obtained by performing the nuclear-structure study. We start from the best-fit mass-mixing matrix presented in [31] and, for comparison, we have considered other estimates of the mixing matrix, i.e., the form written in terms of the mixing angle of solar neutrinos, and the estimation based on a maximum-mixing scheme [23].

In the first part of the paper we review the basic elements of the theory and discuss the structure of the adopted neutrino mass-mixing matrix. We discuss a way to extract light-neutrino masses (m_i) from the observed mass differences and by combining them with the adopted neutrino mass-mixing matrix we calculate the effective neutrino mass relevant for the $0\nu\beta\beta$ decay. In the second part of the paper we review the current nuclear structure information about the $0\nu\beta\beta$ decay, by presenting the up-to-date values of the effective neutrino mass extracted from the adopted limits on the half-lives. In doing so, we have considered the range of variation for the nuclear matrix elements, calculated within definite classes of models. We have focused our attention in the case of the $0\nu\beta\beta$ decay of ^{76}Ge . The nuclear structure analysis includes the values of the nuclear matrix elements reported during last years. We are also presenting a set of nuclear matrix elements, which we have calculated as it is explained in the text. Finally, we discuss the observability of planned experiments on the $0\nu\beta\beta$ decay in the context of the present results.

2. Formalism

2.1. Neutrino data

Two- and three-generation analysis of neutrino data, provided by the solar and atmospheric observations and by the range of mass differences explored in reactor-based experiments, have been performed by several groups [6–11]. The picture which emerges

Table 1

Current limits on neutrino-mass differences. The values listed are a compilation of the results from the SNO [1], SK [2], KamLAND [3] and WMAP [5]

$\delta m_{12}^2 = \delta m_{\text{solar}}^2$	$5 \times 10^{-5} \text{ eV}^2 \rightarrow 1.1 \times 10^{-4} \text{ eV}^2$
$\delta m_{23}^2 = \delta m_{\text{atm}}^2$	$10^{-3} \text{ eV}^2 \rightarrow 5 \times 10^{-3} \text{ eV}^2$
$\sin^2 2\theta_{\text{solar}}$	≈ 0.86
$\sin^2 2\theta_{\text{atm}}$	≈ 1.0
Ω_{ν}	$< 0.71 \text{ eV}$

from these very detailed analysis of neutrino-flavor oscillations favors the large mixing angle (LMA) solution of the Mikheev–Smirnov–Wolfsenstein (MSW) mechanism [15]. Recently, KamLAND Collaboration [3] has confirmed the LMA solution and a crucial step towards the elucidation of the neutrino-mass spectrum was given by the results of WMAP [5,24], which fixed a stringent upper limit for the scale of neutrino masses.² A brief compilation of the adopted results is given in Table 1. As shown in this table, the SNO data are consistent with a value of the mass difference Δm_{12}^2 of the order of 10^{-5} eV (solar-neutrino data), and another independent scale $\Delta m_{31}^2 \approx \Delta m_{32}^2$, of the order of 10^{-3} eV , has been determined from the analysis of the atmospheric-neutrino data, which is in the range of the sensitivity of the reactor-based measurements. Because of the independence of the determined mass differences, the global picture is consistent with the existence of three active neutrino flavors. To these data, the information obtained by WMAP is adding the value of the upper limit of the sum of the three mass eigenvalues (light-neutrino masses only), which is of the order of 0.71 eV [5].

To calculate effective neutrino properties, like the effective electron–neutrino mass, $\langle m_{\nu} \rangle$, one needs to know the neutrino-mixing matrix U and the light-neutrino mass spectrum (m_1, m_2, m_3) [16]. The determination of the matrix elements of U and the absolute values of the masses is the ultimate goal of any of the models of the neutrino and it is, of course, a matter of intensive effort. Out of the very rich, recently published list of articles dealing with the analysis of the SNO results, we have selected two representative ones, namely (a) the results presented in the paper of Bandyopadhyay, Choubey, Goswami and Kar (BCGK) [31], and (b) the expression of the mixing matrix in terms of the solar-neutrino data, and the zeroth-order approximation of the mixing matrix assuming maximum mixing, to perform our calculations. Our choice is motivated by the fact that in the BCGK paper the best-fit value of U , with respect to the solar, atmospheric, and CHOOZ data, is given explicitly and the confidence level of the results is well established. The mixing matrices of case (b) give complementary mixing information and show up in our final results as deviations from the best-fit BCGK-based results.

² The results of WMAP are related to the value of the density of neutrinos in the Universe and not directly to the neutrino mass. Thus, one should use this information with some caution.

The three-generation mixing matrix U can be written as.³

$$U = \begin{pmatrix} c_{13}c_{12} & s_{12}c_{13} & s_{13} \\ -s_{12}c_{23} - s_{23}s_{13}c_{12} & c_{23}c_{12} - s_{23}s_{13}s_{12} & s_{23}c_{13} \\ s_{23}s_{12} - s_{13}c_{23}c_{12} & -s_{23}c_{12} - s_{13}s_{12}c_{23} & c_{23}c_{13} \end{pmatrix}. \tag{1}$$

This expression does not include CP violation, as explained in [31]. By performing a three-generation χ^2 -analysis of the solar-neutrino and CHOOZ data, and by considering the mass differences $\Delta m_{12}^2 = \Delta m_{\text{solar}}^2$, $\Delta m_{31}^2 \approx \Delta m_{32}^2 = \Delta m_{\text{atm}}^2$, the BCGK found that the best fit occurs in the LMA region with $\tan^2 \theta_{13} \approx 0$. This finding greatly simplifies the form of the mixing matrix U , because it narrows the value of U_{e3} down to a very small range around $U_{e3} \approx 0$ [23,31]. The best-fit form of U , reported in the BCGK paper, is

$$U = \begin{pmatrix} 2\sqrt{\frac{2}{11}} & \sqrt{\frac{3}{11}} & 0 \\ -\sqrt{\frac{3}{22}} & \frac{2}{\sqrt{11}} & \frac{1}{\sqrt{2}} \\ \sqrt{\frac{3}{22}} & -\frac{2}{\sqrt{11}} & \frac{1}{\sqrt{2}} \end{pmatrix}. \tag{2}$$

In our second choice for the matrix U we consider $U_{e3} = 0$ and exploit the solar and atmospheric mixing-angles data, reducing Eq. (1) to

$$U = \begin{pmatrix} c_{12} & s_{12} & 0 \\ -s_{12}c_{23} & c_{23}c_{12} & s_{23} \\ s_{23}s_{12} & -s_{23}c_{12} & c_{23} \end{pmatrix}. \tag{3}$$

As a special case of Eq. (3) we have the maximum mixing ($\sin \theta_{12} = \cos \theta_{23} = 1/\sqrt{2}$) solution

$$U = \begin{pmatrix} \frac{1}{\sqrt{2}} & \frac{1}{\sqrt{2}} & 0 \\ -\frac{1}{2} & \frac{1}{2} & \frac{1}{\sqrt{2}} \\ \frac{1}{2} & -\frac{1}{2} & \frac{1}{\sqrt{2}} \end{pmatrix}. \tag{4}$$

Only the first row in the matrices Eqs. (2)–(4) is relevant for the electron–neutrino mass.

The next step consists of the definition of a neutrino mass spectrum. The relative order between the mass eigenvalues, usually referred to in the literature as *mass hierarchy* or *hierarchical order of the mass eigenvalues*, cannot be fixed only by the measured squared mass differences. In order to estimate the possible range of the m_i , we define the relative scales

$$m_1 = f m_2, \quad m_2 = g m_3 \tag{5}$$

for the so-called normal hierarchy ($m_1 \approx m_2 < m_3$), and

$$m_1 = f m_2, \quad m_3 = g m_1 \tag{6}$$

³ This expression does not include CP violation. For the $0\nu\beta\beta$ decay only the first row of the matrix is relevant. Out of the three CP-violating phases (one Dirac phase, two Majorana phases), which are normally included in the matrix, the Dirac phase disappears if $s_{13} = 0$, and the remaining two Majorana phases reduce into one relative phase between the first and second elements of the first row.

for the so-called inverse ($m_1 \approx m_2 > m_3$) and degenerate ($m_3 \approx m_2 \approx m_1$) hierarchies. To these factors we have added the information related to the scale of the mass eigenvalues, which is determined by the extreme value

$$m_0 = \frac{\Omega_\nu}{3}, \quad (7)$$

where the value of Ω_ν is taken from the WMAP data (see Table 1). The factors f and g are determined in such a way that the resulting masses $m_i(f, g)$ obey the observed mass differences, hereafter denoted as Δm^2 ($\Delta m_{31}^2 \approx \Delta m_{32}^2$) and δm^2 (Δm_{12}^2). We are restricted to light-neutrino masses, as said before. The numerical analysis was performed by assuming the above given scalings and by finding the values of (f, g) which are solutions of the equations

$$\frac{1}{1-g^2} - \frac{r}{1-f^2} = 1 \quad (8)$$

for the normal mass spectrum, and

$$\frac{r}{1-f^2} - \frac{1}{1-g^2} = r \quad (9)$$

for the inverse and degenerate cases. The use of the scale m_0 fixes the limiting values of f and g at

$$\begin{aligned} 0 \leq f &\leq \sqrt{1 - \frac{\delta m^2}{g^2 m_0^2}}, \\ 0 \leq g &\leq \sqrt{1 - \frac{\Delta m^2}{m_0^2}} \end{aligned} \quad (10)$$

for the normal hierarchical order,

$$0 < f \leq \frac{1}{\sqrt{1 + \delta m^2/m_0^2}}, \quad 0 \leq g \leq \sqrt{1 - \frac{\Delta m^2}{m_0^2}} \quad (11)$$

for the inverse mass spectrum, and

$$0 < f \leq \frac{1}{\sqrt{1 + \delta m^2 g^2/m_0^2}}, \quad 0 < g \leq \frac{1}{\sqrt{1 + \Delta m^2/m_0^2}} \quad (12)$$

for the nearly degenerate masses.

In the above expressions the factor r is given by the ratio between the solar and atmospheric squared mass differences

$$r = \frac{\delta m^2}{\Delta m^2}. \quad (13)$$

Therefore, the variation of the parameters f and g is effectively restricted by the actual value of r and m_0 . For each set of allowed values of (f, g) and for each of the hierarchies

considered we have calculated m_i . The effective neutrino mass $\langle m_\nu \rangle$, relevant for the $0\nu\beta\beta$ decay, is given by [17–20]

$$\langle m_\nu \rangle_\pm = \sum_{i=1}^3 m_i \lambda_i |U_{ei}|^2 = m_1 U_{e1}^2 \pm m_2 U_{e2}^2, \tag{14}$$

since for the adopted best fit $U_{e3} \approx 0$ [31]. We have consistently neglected CP-violating phases, assumed CP conservation, and written $\lambda_i = \pm 1$, for the relative Majorana phases, since the fit of [31] was performed under the assumption of CP conservation.

This may be considered as a first step towards a more elaborate analysis which should necessarily include the possibility of CP violation. For the purpose of the present work we shall limit ourselves to the case of CP conservation and leave the complete analysis, including also CP violation, for a future effort. In Table 2 we give, for each of the adopted forms of the mixing matrix U , the range of values of the calculated effective electron–neutrino masses. These values correspond to the limiting values of f and g , given in the previous Eqs. (10)–(12). As can be seen from this table, the largest value which one can obtain for $\langle m_\nu \rangle$ is of the order of 0.24 eV, and the smallest one is of the order of 0.7×10^{-4} eV, both for the degenerate mass spectrum. Notice that the larger value is of the order of the mass scale extracted from the results of WMAP and it will certainly depend upon new results for Ω_ν . A value of $\Omega_\nu < 0.5$ eV [24] would then give a mass limit of the order of 0.16 eV, while the estimate $\Omega_\nu < 0.18$ eV [12] will reduce it to the more stringent limit of 0.06 eV. This part of the analysis is, of course, relevant for the present study since it determines exclusion regions for the allowed values of the effective neutrino mass relevant for the $0\nu\beta\beta$ (see, for instance, [11] for a similar approach).

Table 2

Calculated effective electron–neutrino masses $\langle m_\nu \rangle_\pm$. Indicated in the table are the mass spectrum and the adopted mixing matrix. The values are given in units of eV. The results listed as extreme have been obtained by using the extreme upper values of f and g of Eqs. (10)–(12). The adopted values for the mass differences are $\delta m^2_{12} = 7.1 \times 10^{-5}$ eV², $\delta m^2_{23} = 2.7 \times 10^{-3}$ eV², and $m_0 = 0.24$ eV. The mixing matrix $U(a)$ is taken Eq. (2) (the best fit of [31]), $U(b)$ is based on Eq. (3) by taking the largest values of the solar and atmospheric mixing angles, and $U(c)$ is the maximum-mixing solution given explicitly in Eq. (4)

Mass spectrum		$\langle m_\nu \rangle$	$U(a)$	$U(b)$	$U(c)$
Normal	$(m_1 = 0)$	$\langle m_\nu \rangle_-$	−0.010	−0.012	−0.019
		$\langle m_\nu \rangle_+$	0.011	0.012	0.019
	(extreme)	$\langle m_\nu \rangle_-$	0.105	0.086	-0.769×10^{-4}
		$\langle m_\nu \rangle_+$	0.231	0.231	0.231
Inverse	$(m_3 = 0)$	$\langle m_\nu \rangle_-$	0.105	0.087	-0.153×10^{-2}
		$\langle m_\nu \rangle_+$	0.234	0.235	0.235
	(extreme)	$\langle m_\nu \rangle_-$	0.108	0.088	-0.749×10^{-4}
		$\langle m_\nu \rangle_+$	0.237	0.237	0.237
Degenerate	(extreme)	$\langle m_\nu \rangle_-$	0.107	0.088	-0.715×10^{-4}
		$\langle m_\nu \rangle_+$	0.237	0.237	0.237

2.2. Nuclear matrix elements

The implication of these results for $\langle m_\nu \rangle$ upon the rates of $0\nu\beta\beta$ decay is easily seen if one writes⁴ the corresponding half-life, $t_{1/2}^{(0\nu)}$, as

$$(t_{1/2}^{(0\nu)})^{-1} = \left(\frac{\langle m_\nu \rangle}{m_e} \right)^2 C_{mm}^{(0\nu)}, \quad (15)$$

where the factor $C_{mm}^{(0\nu)}$ is defined as

$$C_{mm}^{(0\nu)} = G_1^{(0\nu)} (M_{GT}^{(0\nu)} (1 - \chi_F))^2, \quad (16)$$

in terms of the nuclear matrix elements, $M_{GT}^{(0\nu)} (1 - \chi_F)$, and the phase-space factors, $G_1^{(0\nu)}$, entering the mass term of the transition probability [17].

There are several aspects concerning Eq. (15) which are worth of mentioning:

- (a) in the event of a successful measurement of $0\nu\beta\beta$ decay and considering the information emerging from neutrino-related measurements, Eq. (15) may be viewed as a possible test for nuclear models, since the calculated matrix elements reside in the factor $C_{mm}^{(0\nu)}$;
- (b) if one assigns a certain confidence level to nuclear-structure calculations, by fixing the value of $C_{mm}^{(0\nu)}$, and takes the range of values of the effective neutrino mass extracted from neutrino-related measurements, Eq. (15) may be viewed as a criterium for determining the observability of $0\nu\beta\beta$ decay;
- (c) in the event of a positive measurement of $0\nu\beta\beta$ decay and considering a reliable estimate of the nuclear matrix elements, Eq. (15) may be viewed as a consistency equation for the value of the effective neutrino mass seen in double-beta-decay as compared with the one extracted from neutrino-related experiments.

Let us start with the discussion of the nuclear-structure related information, contained in $C_{mm}^{(0\nu)}$. The ultimate goal of nuclear-structure models is, in fact, the prediction of observables based on the knowledge about nuclear wave functions at the needed level of accuracy. In the case of $0\nu\beta\beta$ decay studies, to achieve this ultimate goal one needs to fulfill several requirements, some of which are purely technical and some of which are conceptual. Among the technical barriers one has, of course, the un-feasibility of large-scale shell-model calculations, prohibited by hardware constraints. Among the conceptual requirements one has the realization that a prediction of a neutrinoless double-beta-decay rate should always be accompanied by other model predictions, like single-beta-decay, electromagnetic and particle-transfer transitions involving the nuclei which participate in the double-beta-decay transition under consideration. We stress the point that, in our experience, the study should be conducted on the basis of a case-by-case analysis.

⁴ Only the mass sector of the half-life will be considered in the following analysis. The expression of the half-life, including right-handed currents, can be found in [17].

Most of the current nuclear-structure approximations are based on the proton–neutron quasiparticle random phase approximation (pnQRPA). This is a framework where proton–neutron correlations are treated as basic building blocks to describe the nuclear states which participate in a double-beta-decay transition. The pnQRPA formalism is rather well known and it has been discussed in a large number of publications during the last forty years. For the sake of brevity we are not going to present it here again, rather we would like to refer the reader to [17] for details. In particular, the sensitivity of the pnQRPA method to values of specific parameters of the interactions, like the sensitivity to the renormalization of the particle–particle (proton–neutron) coupling, has been a matter of intensive studies. Again, we would like to refer to [17] for details concerning this point as well as concerning the large number of extensions of the pnQRPA method, their successes and failures. Restricting ourselves to a very elementary theoretical background, we can say that the standard procedure, applied in the literature to calculate the $0\nu\beta\beta$ -decay rate, involves three major components:

- (a) the calculation of the spectrum of the intermediate double-odd-mass nucleus with $(A, N \pm 1, Z \mp 1)$ nucleons. The pnQRPA is an approximate diagonalization in the one-particle–one-hole, $1p-1h$, (or two-quasiparticle) space and it includes the effects of $2p-2h$ ground-state correlations by means of the backward-going amplitudes. Since the calculations are based on a quasiparticle mean field one forces the breaking of certain symmetries, like the particle-number symmetry by the use of the BCS approximation, and the isospin symmetry, by the use of effective proton and neutron single-particle states. The final results of the pnQRPA calculations will certainly be affected by these symmetry-breaking effects induced by the way in which we handle the nuclear interactions. Some attempts to cure for these effects have been implemented by means of enlarging the representation space, including Pauli-principle-related blocking and by performing self-consistent approaches beyond the quasiparticle mean field. As said before, the list of various extensions of the standard pnQRPA is too long to be commented here in detail. A fairly complete list of references about the set of extensions of the pnQRPA is given in [17–19]. We will generally refer to these approximations as pnQRPA-related ones. In this paper we shall show the results based on this family of approximations.⁵ In addition, we quote the results of the available shell-model calculations;
- (b) the calculation of the leptonic phase-space factors, as dictated by the second-order perturbative treatment of the electroweak interaction. At the level of the minimal extension of the Standard Model (SM) Lagrangian (mass sector only), these phase-space factors can be easily calculated, and the values of them should be rather universal causing no source of discrepancies in the calculations, except for the adopted value of the axial-vector coupling g_A . At the level of the two-nucleon mechanism this value is currently fixed at $g_A = 1.254$ but for the medium-heavy and heavy nuclei an effective

⁵ We shall explicitly quote the sources from where the results have been taken in order to avoid here a repetition of the details of each formalism, since the aim of the present section is not to present a critical review of the theories but rather to show their results to give an idea about the spread in the values of the relevant nuclear matrix elements.

value of $g_A = 1.0$ has also been used. In this work we adopt the conservative estimate of $g_A = 1.254$. Expressions for the phase-space factors, for theories beyond the minimal extension of the SM Lagrangian, i.e., for left–right and right–right couplings, have been listed exhaustively in the literature (see, e.g., [17,18]) and their values are well defined, too. In going beyond the two-nucleon mechanism one has to consider, also, the momentum dependence of the operators, which will reflect upon the structure of the phase-space factors. This is also true for the case of calculations where one is including p-electron wave effects and/or forbidden decays;

- (c) the calculation of the matrix elements of the relevant current operators which act upon the nucleons. These operators are also well known and their multipole structures are derived from the expansion of the electroweak current [17]. In the present calculation we have considered the standard type of operators, without introducing any momentum dependence in them, as originating from the electroweak decay at the quark level [32].

A compilation of the values of nuclear matrix elements and phase-space factors can be found in [17]. The current information about the status of $0\nu\beta\beta$ decays is reported in [33–37].

Tables 3 and 4 show the set of double-beta-decay systems where experimental searches for signals of the $0\nu\beta\beta$ are conducted at present or planned for the next generation of double-beta-decay experiments. The tables contain the experimental lower limits for the $0\nu\beta\beta$ half-life [38–47], the full range of variation of the nuclear matrix elements, as contained in the factors $C_{mm}^{(0\nu)}$ and as they are predicted by different models [17], the values of the model-dependent factor [17]

$$F_N = t_{1/2}^{(0\nu)} C_{mm}^{(0\nu)} = \left(\frac{\langle m_\nu \rangle}{m_e} \right)^{-2}, \quad (17)$$

the calculated phase-space factors $G_1^{(0\nu)}$, and the extracted values of the upper limits the effective neutrino mass.

In Table 4 only a sub-group of calculations are presented, namely the ones based on the plain spherical pnQRPA approach of [17] (third column). These results are compared with our present calculations shown in the fourth column.

In the following, some brief details about the present pnQRPA calculations are given. They have been done by following the procedure outlined in [17]. The two-body nuclear interactions were constructed by using the G -matrix interaction of the Bonn type including two to three major harmonic-oscillator shells around the proton and neutron Fermi surfaces. The spherical Woods–Saxon potential was used to generate the single-particle energies and small adjustments of these energies were done in the vicinity of the Fermi surfaces to reproduce the low-energy quasiparticle spectra of the neighboring odd-mass nuclei. Following the criteria which we have advanced above, the various parameters involved in the calculations have been fixed by reproducing the known data on single-beta-decay transitions around the nuclei of interest for the double-beta-decay transitions which we are considering here. No further adjustment of the proton–neutron particle–particle coupling constant [17] is introduced once the known single-beta-decay observables are reasonably reproduced.

Table 3

$0\nu\beta\beta$ model-dependent estimates and experimental limits. The double-beta-decay systems are given in the first column. The factors $C_{mm}^{(0\nu)}$ are given in units of yr^{-1} and their values are shown within the intervals predicted by different nuclear-structure models, like the shell model (a), the quasiparticle random phase approximation (b), the pseudo SU(3) model (c), and various other models (d). The value $g_A = 1.254$ is used. The quantities $t_{1/2}^{(0\nu)}$ are the experimental lower limits of the half-lives, in units of years. The corresponding references are quoted in brackets. The factor F_N (lower limit) is shown in the fourth column and the values are given within the intervals provided by the factors $C_{mm}^{(0\nu)}$. The last column shows the range of variation of the extracted upper limits for the effective neutrino mass (upper limits) in units of eV. The coefficients $C_{mm}^{(0\nu)}$ are taken from [17], except for the case of ^{124}Sn [59]

System	$C_{mm}^{(0\nu)}$	$t_{1/2}^{(0\nu)}$	F_N (min)	$\langle m_\nu \rangle_{\text{max}}$
^{48}Ca	$(1.55\text{--}4.91) \times 10^{-14}$ (a) $(9.35\text{--}363) \times 10^{-15}$ (b)	9.5×10^{21} [38]	$(1.47\text{--}4.66) \times 10^8$ $(8.88\text{--}345) \times 10^7$	$(23.7\text{--}42.1)$ $(8.70\text{--}54.2)$
^{76}Ge	$(1.42\text{--}28.8) \times 10^{-14}$ (d)	2.5×10^{25} [29]	$(3.55\text{--}72.0) \times 10^{11}$	$(0.19\text{--}0.86)$
^{82}Se	$(9.38\text{--}43.3) \times 10^{-14}$ (d)	2.7×10^{22} [40]	$(2.53\text{--}11.7) \times 10^9$	$(4.73\text{--}10.2)$
^{96}Zr	$(9.48\text{--}428) \times 10^{-15}$ (b)	1.0×10^{21} [41]	$(9.48\text{--}428) \times 10^6$	$(24.7\text{--}166)$
^{100}Mo	$(0.07\text{--}2490) \times 10^{-15}$ (b)	5.5×10^{22} [42]	$(0.38\text{--}13700) \times 10^7$	$(1.38\text{--}262)$
^{116}Cd	$(5.57\text{--}66.1) \times 10^{-14}$ (b)	1.3×10^{23} [43]	$(3.90\text{--}46.3) \times 10^9$	$(2.37\text{--}8.18)$
^{124}Sn	$(2.29\text{--}5.70) \times 10^{-13}$ (b)	2.4×10^{17} [44]	$(5.50\text{--}13.7) \times 10^4$	$(1.38\text{--}2.18) \times 10^3$
^{128}Te	$(1.71\text{--}33.6) \times 10^{-15}$ (b)	8.6×10^{22} [45]	$(1.47\text{--}28.9) \times 10^8$	$(9.51\text{--}42.1)$
^{130}Te	$(1.24\text{--}5.34) \times 10^{-13}$ (b)	2.1×10^{23} [45]	$(1.74\text{--}7.48) \times 10^{10}$	$(1.87\text{--}3.87)$
^{136}Xe	$(2.48\text{--}15.7) \times 10^{-14}$ (a), (b)	4.4×10^{23} [46]	$(1.09\text{--}6.91) \times 10^{10}$	$(1.94\text{--}4.89)$
^{150}Nd	$(4.78\text{--}77.4) \times 10^{-13}$ (b), (c)	1.7×10^{21} [47]	$(8.13\text{--}132) \times 10^8$	$(4.45\text{--}17.9)$

Table 4

Calculated phase-space factors $G_1^{(0\nu)}$ and calculated nuclear matrix elements, using the formalism of the spherical pnQRPA, for some of the double-beta emitters included in Table 3. The phase space factors are given in units of yr^{-1} and the dimensionless matrix elements are scaled by the nuclear radius [17]. Note that for the case of ^{100}Mo the present (correct) value of the phase space factor differs from the one (a misprint) given in [17]. The third column, indicated as N.M.E., gives the extreme values of the nuclear matrix elements $M_{\text{GT}}^{0\nu}(1 - \chi_F)$ reported in the literature (see the captions to Table 3), and the fourth column, indicated as N.M.E. (this work), gives the results of the present calculations for $M_{\text{GT}}^{0\nu}(1 - \chi_F)$. The last column shows the range of values of the upper limit for the effective neutrino mass, in units of eV, extracted from the results given in the third and fourth columns

System	$G_1^{(0\nu)} \times 10^{14}$	N.M.E.	N.M.E. (this work)	$\langle m_\nu \rangle_{\text{max}}$
^{48}Ca	6.43	1.08–2.38		8.70–19.0
^{76}Ge	0.63	2.98–4.33	3.33	0.30–0.43
^{82}Se	2.73	2.53–3.98	3.44	4.73–7.44
^{96}Zr	5.70	2.74	3.55	19.1–24.7
^{100}Mo	4.57	0.77–4.67	2.97	2.18–13.2
^{116}Cd	4.68	1.09–3.46	3.75	2.37–8.18
^{128}Te	0.16	2.51–4.58		9.51–17.4
^{130}Te	4.14	2.10–3.59	3.49	1.87–3.20
^{136}Xe	4.37	1.61–1.90	4.64	0.79–2.29

As one can see, our present results are in good agreement with the other pnQRPA calculations, except for ^{136}Xe where our calculation gives a larger matrix element than the other calculations. This deviation might occur due to the semi-magic nature (the neutron

shell is closed) of ^{136}Xe , forcing the transition from the two-quasiparticle description to the particle–hole description.

If one compares the extracted upper limits for the neutrino masses of Table 3 with the ranges of neutrino masses given in the previous section, it becomes evident that the present generation of $0\nu\beta\beta$ experiments is rather insensitive to the effective neutrino mass coming from the best fit of the solar + atmospheric + reactor data, except for the Heidelberg–Moscow experiment if one takes the range of values ($\langle m_\nu \rangle = 0.11\text{ eV}–0.56\text{ eV}$) reported in [27]. If one takes the value ($m_\nu \rangle \approx 0.24\text{ eV}$ (the heaviest possible effective mass), which is favored by the inverse and degenerate mass spectra (see Table 2), one sees that it is outside the range of the present upper limits fixed by double-beta-decay experiments, with the possible exception of the decay of ^{76}Ge , which just barely reaches this estimate. Naturally, the upper limits of $\langle m_\nu \rangle$ extracted from the experimental lower limits of $t_{1/2}^{(0\nu)}$ are model dependent, since the connection between the half-lives and the effective neutrino mass is given by the nuclear-model-dependent factors F_N . As a reference value, for $\langle m_\nu \rangle \approx 0.24\text{ eV}$ one obtains $F_N = 4.53 \times 10^{12}$ (see Eq. (17)) which is to be compared with the estimate (see Table 3, case of ^{76}Ge) $F_N \geq 3.55 \times 10^{11} \rightarrow 7.20 \times 10^{12}$, computed by assuming $t_{1/2}^{(0\nu)} > 2.5 \times 10^{25}\text{ yr}$ [29] and taking into account the total span of the calculated nuclear matrix elements.

With reference to the results shown in Table 4, the span in the upper limits of the effective neutrino mass is smaller, if one takes only the results of the spherical pnQRPA (see the last column of Table 4), than when all the available model calculations are included (see the last column of Table 3). For the case of ^{76}Ge the spherical pnQRPA gives a span of $\langle m_\nu \rangle = 0.30\text{ eV}–0.43\text{ eV}$ in upper limit of the effective mass. This means that to reach the neutrino-mass value resulting from the neutrino data, one definitely needs larger matrix elements than the ones produced thus far by the spherical pnQRPA model, and/or longer half-lives than the present measured limits. These observations will be discussed in detail in the next section.

2.3. pnQRPA matrix elements for ^{76}Ge

Table 5 shows the results of the matrix elements, corresponding to the mass sector of the neutrinoless double-beta decay in ^{76}Ge , calculated within the family of the pnQRPA-related models [48–55]. The standard spherical pnQRPA method gives results which are of the order of $C_{mm}^{(0)} \approx 5–8 \times 10^{-14}$ in units of yr^{-1} , with the exception of the result presented in [55], which yields to a magnitude of the order of $1.85 \times 10^{-14}\text{ yr}^{-1}$, and the one of [48] where the pnQRPA value is $1.12 \times 10^{-13}\text{ yr}^{-1}$. These factors translate into the ranges of the nuclear matrix elements⁶ and upper limits of the effective neutrino masses which were shown, previously, in Tables 3 and 4. The results of the other, pnQRPA-related, approximations seem to be less stable and they deviate more from the central range of $C_{mm}^{(0)} \approx 5–8 \times 10^{-14}\text{ yr}^{-1}$. In analyzing the results of [55] one can notice that the largest value does not differ much from the standard pnQRPA value, although it has been obtained

⁶ Notice that the results of [48], which are relevant for the analysis performed in [27], are only 1.3 times larger than the average pnQRPA matrix element.

Table 5

Calculated nuclear matrix elements for the case of ^{76}Ge . The values $C_{mm}^{(0)}$ are given in units of yr^{-1} . The adopted value for the lower limit of the half-life is the value recommended in [29], $t_{1/2}^{(0\nu)} = 2.5 \times 10^{25}$ yr. Indicated in the table are the models used to calculate the nuclear matrix elements, which are taken from the references quoted in the last row of the table. The abbreviations stand for the proton–neutron quasiparticle random-phase approximation (pnQRPA), particle-number-projected pnQRPA (pnQRPA (proj.)), proton–neutron pairing pnQRPA (pnQRPA + pn pairing), the renormalized pnQRPA (RQRPA), the second pnQRPA (SQRPA), the self-consistent renormalized pnQRPA (SCRQRPA), the fully renormalized pnQRPA (full-RQRPA), and the variation after projection mean-field approach (VAMPIR). The model assumptions underlying these theories are presented in the quoted references

$C_{mm}^{(0)}$	$F_N(\text{min}) \times 10^{-12}$	Theory	Refs.
1.12×10^{-13}	2.80	pnQRPA	[48,49]
6.97×10^{-14}	1.74	pnQRPA	[32]
7.51×10^{-14}	1.88	pnQRPA (proj.)	[32]
7.33×10^{-14}	1.83	pnQRPA	[50]
1.42×10^{-14}	0.35	pnQRPA + pn pairing	[50]
1.18×10^{-13}	2.95	pnQRPA	[51]
8.27×10^{-14}	2.07	pnQRPA	[52]
2.11×10^{-13}	5.27	RQRPA	[53]
6.19×10^{-14}	1.55	RQRPA + q-dep. operators	[53]
$1.8\text{--}2.2 \times 10^{-14}$	0.45–0.55	pnQRPA	[54]
$5.5\text{--}6.3 \times 10^{-14}$	1.37–1.57	RQRPA	[54]
$2.7\text{--}3.2 \times 10^{-15}$	0.07–0.08	SCRQRPA	[54]
1.85×10^{-14}	0.46	pnQRPA	[55]
1.21×10^{-14}	0.30	RQRPA	[55]
3.63×10^{-14}	0.91	full-RQRPA	[55]
6.50×10^{-14}	1.62	SQRPA	[55]
2.88×10^{-13}	7.20	VAMPIR	[56]
1.58×10^{-13}	3.95	Shell Model	[57]
1.90×10^{-14}	0.47	Shell Model	[58]

by using a more involved approximation. By using the phase-space factors listed in Table 4, we arrive at the central value for the matrix elements in the pnQRPA, namely

$$M_{\text{GT}}^{(0\nu)}(1 - \chi_{\text{F}})_{\text{pnQRPA}} = 3.65. \tag{18}$$

The corresponding value for the latest large-scale shell-model calculation [58] is given by

$$M_{\text{GT}}^{(0\nu)}(1 - \chi_{\text{F}})_{\text{shell-model}} = 1.74. \tag{19}$$

Therefore, the latest shell-model results [58] and the centroid of the pnQRPA results differ by a factor of the order of 2. In terms of the effective neutrino mass, using the half-life $t_{1/2}^{(0\nu)} \geq 2.5 \times 10^{25}$ yr recommended in [29], these matrix elements lead to

$$\langle m_\nu \rangle_{\text{pnQRPA}} \leq 0.35 \text{ eV}, \tag{20}$$

for the pnQRPA estimate, and

$$\langle m_\nu \rangle_{\text{shell-model}} \leq 0.74 \text{ eV}, \tag{21}$$

for the shell-model estimate of the matrix element. It means that to go to masses of the order of 0.24 eV, as required by WMAP, one needs larger nuclear matrix elements than

the ones given by the pnQRPA or by the available shell-model results. In fact, to reach the WMAP limit one would need the value

$$M_{\text{GT}}^{(0\nu)}(1 - \chi_{\text{F}})_{\text{experimental}} \geq 5.36, \quad (22)$$

which is $\approx \sqrt{2}$ times larger than the reference pnQRPA value given in (18). The largest matrix element listed in Table 5, coming from the VAMPIR approach [56], would yield to the value $\langle m_\nu \rangle_{\text{VAMPIR}} \leq 0.19$ eV, which just touches the value $\langle m_\nu \rangle \leq 0.24$ eV coming from the analysis of the neutrino-related data. However, it is appropriate to point out here that the VAMPIR matrix element is to be considered unrealistically large because in the calculations of [56] no proton–neutron residual interaction was included.

Finally, our present value

$$M_{\text{GT}}^{(0\nu)}(1 - \chi_{\text{F}})_{\text{pnQRPA}}^{\text{present}} = 3.33 \quad (23)$$

(see Table 4) is consistent with the central value (18), and it yields an effective neutrino mass

$$\langle m_\nu \rangle_{\text{pnQRPA}}^{\text{present}} \leq 0.39 \text{ eV} \quad (24)$$

if one takes for the half-life the lower limit recommended in [29], and

$$\langle m_\nu \rangle_{\text{pnQRPA}}^{\text{present}} \leq 0.50 \text{ eV} \quad (25)$$

if one takes for the half-life the value 1.5×10^{25} yr given by Heidelberg–Moscow Collaboration [27].

3. Observability of the neutrinoless double beta decay

To grasp an idea about the observability of the $0\nu\beta\beta$ decay in other systems, we can compare the values of F_N , of Table 3, with the ones obtained by using the upper limit of the effective neutrino mass of 0.24 eV, corresponding to $F_N \geq 4.53 \times 10^{12}$.

Fig. 1 shows the comparison between the lower limits of the values of F_N of Eq. (18), listed in Table 3, and the values corresponding to the effective neutrino masses $\langle m_\nu \rangle = 0.24$ eV (upper limit coming from the neutrino data) and 0.39 eV (central value reported in [27]). The interval between upper and lower values, for each case, represents the span of the calculated nuclear matrix elements. For the case of ^{76}Ge the prominent upper value is given by the unrealistically large nuclear matrix element of [56].

The results shown in Fig. 1 indicate a departure with respect to the experimental limits by orders of magnitude, excluding the case of ^{76}Ge which is closer but still outside of the range consistent with the solar + atmospheric + reactor neutrino data.

Thus the issue about the observability of the $0\nu\beta\beta$ decay relies, from the theoretical side, upon the estimates for the effective neutrino mass and upon the estimates of the relevant nuclear matrix elements. While in some cases the differences between the calculated matrix elements are within factors of the order of 3, in some other cases the differences are much larger. It shows one of the essential features of the nuclear double-beta decay, namely that case-by-case theoretical studies are needed instead of a global one [17]. The elucidation of

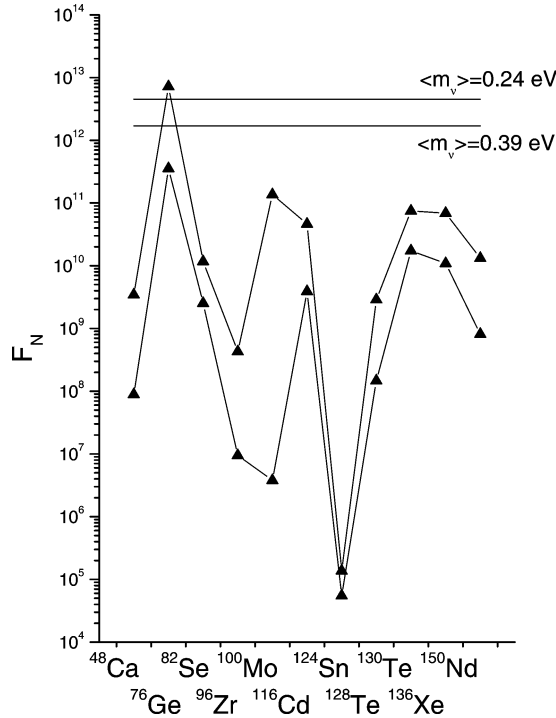


Fig. 1. Factors $F_N(\min)$, of Eq. (18), for each of the systems of Table 3. The lines are drawn to guide the eye. The interval between the upper and lower lines, for each case, represents the span of the calculated nuclear matrix elements. The results corresponding to $\langle m_\nu \rangle = 0.24 \text{ eV}$ and $\langle m_\nu \rangle = 0.39 \text{ eV}$ are shown as horizontal lines.

this problem relies on data which may be available in the next generation of double-beta-decay experiments. These future experiments are needed to reach the values of effective neutrino masses extracted from the neutrino-oscillation-related data.

4. Conclusions

To conclude, in this paper we have presented results on the effective neutrino mass, as obtained from the best-fit mass-mixing matrix U determined from the analysis of solar + atmospheric + reactor + satellite data, and compared them with the values extracted from neutrinoless double-beta-decay experiments. The analysis of the neutrino sector was performed under the assumption of CP conservation, in a manner consistent with the fit of the mixing matrix, under the constraints for $U_{e3} \approx 0$. A more elaborate one, including CP-violating phases in the neutrino sector will be performed in a subsequent effort.

The value of the effective electron–neutrino mass extracted from the neutrino-related experiments, $\langle m_\nu \rangle \leq 0.24 \text{ eV}$, does not compare with the central value of $\langle m_\nu \rangle \approx 0.39 \text{ eV}$, reported in [27] and obtained by using the nuclear matrix elements calculated in [48]. It

does not compare, either, with the values given by the standard pnQRPA model, after taking into account the span in the calculated matrix elements.

To explain for the difference between the above results, we have compiled a systematics of the calculated nuclear matrix elements and performed additional pnQRPA calculations. In the case of ^{76}Ge , and if one adopts for the half-life the lower limit of 2.5×10^{25} yr suggested in [29], the nuclear matrix elements needed to yield the desired effective neutrino masses are larger than any of the known nuclear matrix elements calculated in the framework of the spherical pnQRPA. This conclusion also holds for the available shell-model results.

The present knowledge of the involved nuclear matrix elements shows that the sensitivity of the $0\nu\beta\beta$ experiments is still far from the estimate coming from neutrino oscillations. However, the needed sensitivity is potentially achievable by the next generation of experiments.

Acknowledgements

This work has been partially supported by the National Research Council (CONICET) of Argentina and by the Academy of Finland under the Finnish Centre of Excellence Programme 2000–2005 (Project No. 44875, Nuclear and Condensed Matter Programme at JYFL). One of the authors (O.C.) gratefully thanks the warm hospitality extended to him at the Department of Physics of the University of Jyväskylä, Finland. The authors are grateful to Profs. A. Barabash, S. Jullian, J. Maalampi, V. Tretyak, Y. Zdesenko and F. Avignone III, for very useful discussions and suggestions concerning the material presented in the manuscript.

References

- [1] SNO Collaboration, Q.R. Ahmad, et al., Phys. Rev. Lett. 87 (2001) 071301;
SNO Collaboration, Q.R. Ahmad, Phys. Rev. Lett. 89 (2002) 011301;
SNO Collaboration, Q.R. Ahmad, Phys. Rev. Lett. 89 (2002) 011302.
- [2] Super-Kamiokande Collaboration, S. Fukuda, et al., Phys. Rev. Lett. 86 (2001) 5651.
- [3] KamLAND Collaboration, K. Eguchi, et al., Phys. Rev. Lett. 90 (2003) 021802.
- [4] M. Appollonio, et al., Phys. Lett. B 466 (1999) 415.
- [5] C.L. Bennet, et al., astro-ph/0302207.
- [6] J.W.F. Valle, hep-ph/0205216, and references therein.
- [7] J.N. Bahcall, M.C. Gonzalez-Garcia, C. Peña-Garay, hep-ph/0204314;
J.N. Bahcall, M.C. Gonzalez-Garcia, C. Peña-Garay, hep-ph/0204194.
- [8] S.R. Elliott, P. Vogel, Annu. Rev. Nucl. Part. Sci. 52 (2002) 115, and references therein.
- [9] S.M. Bilenky, D. Nicclo, S.T. Petcov, hep-ph/0112216.
- [10] K. Cheung, hep-ph/0302265.
- [11] S. Pascoli, S.T. Petcov, W. Rodejohann, hep-ph/0209059;
S. Pascoli, S.T. Petcov, W. Rodejohann, hep-ph/0212113.
- [12] J. Ellis, astro-ph/0204059.
- [13] H. Minakata, H. Sugiyama, hep-ph/0212240.
- [14] G. Bhattacharyya, H. Päs, L. Song, T. Weiler, hep-ph/0302191.
- [15] L. Wolfenstein, Phys. Rev. D 17 (1978) 2369;
S.P. Mikheev, A.Y. Smirnov, Sov. J. Nucl. Phys. 42 (1985) 913.

- [16] A.Y. Smirnov, Czech. J. Phys. 52 (2002) 439.
- [17] J. Suhonen, O. Civitarese, Phys. Rep. 300 (1998) 123.
- [18] J.D. Vergados, Phys. Rep. 361 (2002) 1.
- [19] H. Ejiri, Phys. Rep. 338 (2000) 265.
- [20] A. Faessler, F. Šimkovic, J. Phys. G 24 (1998) 2139.
- [21] H.V. Klapdor-Kleingrothaus, H. Päs, A.Y. Smirnov, Phys. Rev. D 63 (2001) 073005.
- [22] P. Vogel, Phys. Rev. D 66 (2002) 010001.
- [23] E. Ma, hep-ph/0303126.
- [24] A. Pierce, H. Maruyama, hep-ph/0302131.
- [25] H.V. Klapdor-Kleingrothaus, U. Sarkar, Mod. Phys. Lett. 16 (2001) 2469.
- [26] H.J. He, D.A. Dicus, J.N. Ng, hep-ph/0203237.
- [27] H.V. Klapdor-Kleingrothaus, A. Dietz, H.L. Harney, I.V. Krivosheina, Mod. Phys. Lett. A 16 (2001) 2409; H.V. Klapdor-Kleingrothaus, et al., Part. Nucl., Lett. 1 (2002) 57.
- [28] C.E. Aalseth, et al., hep-ph/0202018, Mod. Phys. Lett. A 17 (2002) 1475.
- [29] Yu.G. Zdesenko, F.A. Danevich, V.I. Tretyak, Phys. Lett. B 546 (2002) 206.
- [30] F. Feruglio, A. Strumia, F. Vissani, Nucl. Phys. B 637 (2002) 345.
- [31] A. Bandyopadhyay, S. Choubey, S. Goswami, K. Kar, hep-ph/0110307.
- [32] J. Suhonen, O. Civitarese, A. Faessler, Nucl. Phys. A 543 (1992) 645.
- [33] Y. Zdesenko, Rev. Mod. Phys. 74 (2002) 663.
- [34] V.I. Tretyak, Yu.G. Zdesenko, At. Data Nucl. Data Tables 61 (1995) 43.
- [35] F.A. Danevich, et al., Phys. At. Nucl. 59 (1996) 1.
- [36] V.I. Tretyak, Yu.G. Zdesenko, At. Data Nucl. Data Tables 80 (2002) 83.
- [37] A.S. Barabash, Czech. J. Phys. 52 (2002) 567.
- [38] K. You, et al., Phys. Lett. B 265 (1991) 53.
- [39] L. Baudis, et al., Phys. Rev. Lett. 83 (1999) 41.
- [40] S.R. Elliot, et al., Phys. Rev. C 46 (1992) 1535.
- [41] R. Arnold, et al., Nucl. Phys. A 658 (1999) 299.
- [42] H. Ejiri, et al., Phys. Rev. C 63 (2001) 065501.
- [43] F.A. Danevich, et al., Phys. Rev. C 62 (2000) 045501; P.G. Bizzeti, et al., Nucl. Phys. B (Proc. Suppl.) 110 (2002) 389.
- [44] M.I. Kalkstein, W.F. Libby, Phys. Rev. 85 (1952) 368.
- [45] A. Alessandrello, et al., Phys. Lett. B 486 (2000) 3319; C. Arnoboldi, et al., Phys. Lett. B 557 (2003) 167.
- [46] R. Luescher, et al., Phys. Lett. B 434 (1998) 407.
- [47] A.A. Klimenko, A.A. Pomansky, A.A. Smolnikov, Nucl. Instrum. Methods B 17 (1986) 445.
- [48] A. Staudt, K. Muto, H.V. Klapdor-Kleingrothaus, Europhys. Lett. 13 (1990) 31.
- [49] K. Muto, E. Bender, H.V. Klapdor-Kleingrothaus, Z. Phys. A 334 (1989) 187.
- [50] G. Pantis, F. Šimkovic, J.D. Vergados, A. Faessler, Phys. Rev. C 53 (1996) 695.
- [51] T. Tomoda, Rep. Prog. Phys. 54 (1991) 53.
- [52] C. Barbero, F. Krmpotic, A. Mariano, D. Tadic, Nucl. Phys. A 650 (1999) 485.
- [53] F. Šimkovic, G. Pantis, J.D. Vergados, A. Faessler, Phys. Rev. C 60 (1999) 055502.
- [54] A. Bobyk, W.A. Kaminski, F. Šimkovic, Phys. Rev. C 63 (2001) 051301(R) .
- [55] S. Stoica, H.V. Klapdor-Kleingrothaus, Nucl. Phys. A 694 (2001) 269.
- [56] T. Tomoda, A. Faessler, K.W. Schmid, F. Grümmer, Nucl. Phys. A 452 (1986) 591.
- [57] W.C. Haxton, G.F. Stephenson Jr., Prog. Part. Nucl. Phys. 12 (1984) 409.
- [58] E. Caurier, F. Nowacki, A. Poves, J. Retamosa, Phys. Rev. Lett. 77 (1996) 1954.
- [59] M. Aunola, J. Suhonen, Nucl. Phys. A 643 (1998) 207.